



Docking Studies on Novel HCVNS5b Inhibitors

KEYWORDS

HCV; RESP; Autodock

Ahmed M El-Nahas

Yasmine S. Moemen

Serry, A. El-Beily

Chemistry Department, Faculty of Science, El-Menoufia University, Shebin El-Kom, Egypt.

National Liver Institute, El-Menoufia University, Shebin El-Kom, Egypt

Pharmaceutical organic Chemistry, Faculty of Pharmacy, Mansoura University, Mansoura, Egypt

ABSTRACT This study elucidates the binding mode of non nucleoside and nucleoside analogue inhibitors to the crystal structure of HCV NS5b, 2HAI, by means of molecular docking. Receptor based approaches were applied to novel ten HCV NS5b inhibitors. Docking protocol with both Restricted Electrostatic Potential (RESP) charge and Gasteiger charges were performed. The docking study confirmed that non-polar hydrophobic (Leu419), polar hydrophilic (Ser 476) and positively charged polar (Arg501) residues are important interaction sites in Thumb domain of the polymerase. These novel compounds show high activity toward allosteric sites and active site, when applying RESP charges for non nucleoside inhibitors and bad influence for nucleoside analogue inhibitors.

Summary

The deprotonated form after applying RESP charges were improved the docking results for compounds 1-5, while worsened for inhibitors 6-10. Compounds 4, 5, 9 are considered as the most active compounds for Thumb pocket-II.

Introduction

Ribavirin, a nucleoside analogue inhibitor, has a wide-ranging antiviral activity (Gilbert & McLeay, 2008; Koren, King, Knowles, & Phillips, 2003; Véronique et al., 2011); this is representing in inhibition of Inosine-5'-monophosphate dehydrogenase (IMP dehydrogenase), which lowers cellular GTP (Chung et al., 2007) with many proposed mechanisms to explain this activity (Bougie & Martin, 2003; Moriyama et al., 2008). Ribavirin targets the polymerase HCV NS5b (Corouge & Pol, 2011; Miles, Miles, Redington, & Eyring, 1976; Yong, 2003), which is responsible for HCV replication (Lee, 2004). It enhances early sustained virological response (SVR) rates during interferon-based antiviral HCV therapy (Hofmann, Herrmann, Sarrazin, & Zeuzem, 2008).

Carboxylic acids such as malic and citric have anticoagulant property and prevent kidney calculi (Moreno-Cid, Yebra, & Santos, 2004). Malic, citric and tartaric are involved in Krebs cycle for energy production in human cell (Shaw, 2008). In addition, such acids or their derivatives introduce potent natural analogue drugs (El Bialy, Holger, & Lutz, 2005; Tietze et al., 2007). Malate derivatives are engaged in inhibition of viral, neoplastic diseases as HBV and HIV (Zhou, Jahansson, & Wahling, 2005).

This study aims at developing novel HCV NS5b for both non-nucleoside and nucleoside analogue inhibitors. They docked into different potential sites with Autodock (Cosconati et al., 2010). Autodock fails to predict the partial charges on both the protein and the ligand, as a consequence it might underestimate the binding energy with about 2-3 Kcal/mol (Cosconati et al., 2010). In an attempt to further improve binding energy prediction, RESP charges were calculated before docking (Wang, Cieplak, & Kollman, 2000).

Methodology

All inhibitors as seen in Fig.1, were optimized by Gaussian03 (Frisch et al.) at B3LYP/6-31G*, ESP charge was calculated at B3LYP/cc-pVTZ and followed by RESP calculations by Antechamber (Case et al., 2010).

Docking was carried out by MGLTools v.1.5.4 (Sanner, 1999) which is an interface for Autodock. Before docking process, for receptor: ligand and water molecules were removed, polar hydrogen atoms and charges were added. Finally, atom

types were assigned on both ligand and receptor. The docking sites were applied as following: Thumb pocket-I (Pro495, Pro496, Val499), Thumb pocket-II (Leu419, Met423), Palm pocket-I (Asn411, Met414, Tyr448) and the active site (Ser 282) (Betzi et al., 2009) with dimensions 126x126x126 Å and also 0.2 Å for grid spacing; the Lamarckian genetic algorithm (LGA) was applied with 100 runs to broaden the search as possible for the most likely conformations and finally docking calculations were performed using Autodock4 (Li et al., 2006). The minimized receptor "2HAI", was redocked to the co-crystal ligand with RMSD = 0.9 Å (Li et al., 2006). Docking was applied twice; one for the neutral and the other for the deprotonated structures due to the activity of the deprotonated forms compared to the neutral ones (Zapata-Torres et al., 2012).

All docking computations were automated by Raccoon, which is a valid tool for virtual screening (Forli, 2010); dockres tool (Mezei & Zhou, 2010) used to extract the best poses for each one of three receptor sites (Thumb pocket-I, II, Palm pocket-I) and the active site. LPC package (Sobolev, Sorokine, Prilusky, Abola, & Edelman, 1999) demonstrated all types of interactions between ligand and receptor with graphic representation by Chimera (Pettersen et al., 2004) and Molegro molecular view (Thomsen & Christensen, 2006).

Results and Discussion

RNA dependent RNA polymerases (RdRP) structure is a right hand conformation, it composed of "fingers", "palm," and "thumb" sub-domains as any DNA-dependent RNA polymerases (Brautigam & Steitz, 1998) as in Fig.2. "The fingers domain is characterized by two regions: an inner region that consists primarily of a bundle of α -helices, surrounding and packed against the palm sub-domain, and an outer region projecting away from the palm". In this region, the nucleotide binding site exists near to the active site. The palm domain is composed of a catalytic active site with highly conserved regions in all RdRP and also among all known template-dependent polynucleotide polymerases (Gorbalenya et al., 2002; O'Reilly & Kao, 1998); the palm domain includes palm I, II, III (Lesburg, Radfar, & Weber, 2000) (Beaulieu, 2009); Because of overlapping of palm I:III (Beaulieu, 2009), we investigated it as one site. The thumb domain is an allosteric binding sites adjacent to GTP with 30 Å away from the catalytic center (Lesburg et al., 2000).

Thumb pocket-I investigations of deprotonated non nucleoside analogues 1-5 showed that the phenol group is directed toward the hydrophobic residues Val494, Leu489 and Ala486, Fig.3. Most of hydroxyl or carbonyl groups exist at the terminal of these structures form hydrogen bonds with different residues: O4 with hydrophobic residues Val 494 as in case of compounds 1-3, O5 with Arg501 for inhibitors 1-3 or with Arg498 for 4-5; O7 with Arg498 for 1-5 and O11 only in compound 5 with Leu497. Also, there is a change in the structure orientation in 4 which might decrease hydrophobicity and binding energy as displayed in Fig. 4.

For nucleoside analogue 6-8, the sugar ring and 1, 2, 4 triazole ring (hydrophobic part) are directed to the hydrophobic residues Val494, Leu489 and Leu497, respectively. The other part of structure is directed toward Arg498 and Arg501 except in 9, 10 where tetrahydrofuran ring is shifted up to Asn28, Ser29 and shifting of 1, 2, 4 triazole to Arg32. Compounds 6-10 form more hydrogen bonds than 1-5. This may due to the sugar ring which increase hydrogen bonds in these compounds and lower binding affinity to be more potent as shown in Fig.4.

For Thumb pocket-II analysis of compounds 1-5, phenol group is pointed to hydrophobic residues Thr418, Leu419 or Arg422, Tyr477 and also form three HB, O3 with Thr418, Leu419, Tyr477 and O4 with Ser476 except compound 5. Compound 4 is considered as the most active inhibitor with binding energy of -10.7 kcal/mol and the highest hydrophobicity with 24 hydrophobic interactions as depicted in Fig.4.

From Palm pocket-I analysis, there is a parallel π - π stacking between Tyr415 and phenol group of inhibitors 1-3. For inhibitors 1-5, there are electrostatic interactions of O7-10 with the surrounding residues Arg386, Thr390, Pro391 and Arg394. For inhibitors 6-10, there are electrostatic interactions between carbonyl groups of O7-10 and Arg390, Pro391 and Arg386.

As displayed in Fig. 4 and Table 1, there is a strong relation between hydrophobicity and binding energy which indicates tendency of compounds 1-5 to bind to allosteric sites and active site as follows: Palm pocket-I > Thumb pocket-II > Thumb pocket-I > Active site. However, from Table 1, we can deduce the following: non nucleoside inhibitors 1-5 are binds weakly to both sites Thumb pocket-I and the active site by $R^2=0.43$, 0.41 while binds strongly to both Thumb pocket-II and Palm pocket-I by $R^2=0.77$ and 0.85 as in case of neutral form. In case of deprotonated form it is strongly bind to Palm pocket-I, Thumb pocket-II and I than the active site. This phenomena can be ascribed to charge improvement over the atoms as found in the literature (Hou, Zhang, & Xu, 2002). In case of nucleoside inhibitors 6-10, using RESP charges worsen the docking results as reported previously (Ryška, 2011)

For compounds 6-10, there is an electrostatic interaction between carbonyl group of O7, O8, O9, O10 and Lys533, Val530, Arg501 as shown in Fig. 3. Compound 9 is the most potent inhibitor as seen in Fig. 4.

Figure 1: The novel ten HCVNS5B inhibitors of the current study.

Figure 2: Represents Compound 1 docked to allosteric sites (Thumb pocket-I, II, Palm pocket-I) and the active site.

Figure 3: schematic representation for Thumb pocket-I,II and Palm pocket-I poses for inhibitor 1-10, while 8 colored white to differentiate between 6,8. Amino acid residues appear as thin sticks while ligand atoms are represented as bold sticks. The hydrophobic parts appear in green while the hydrophilic moieties in orange and gray colors. Hydrophilic residues have a red color, while hydrophobic residues have blue color. Atoms of residues are colored according to the hydrophobicity index proposed by Kyte and Doolittle in 1982 (Kyte & Doolittle,

1982), The blue dashed line represents the hydrogen bond, b. Electrostatic interactions between carbonyl groups and residues surrounding it. The compounds colored according to their atoms, red circles refer to negative charge while blue for positive charge while the inhibitors colored according to their atom types.

Figure 4: Types of intermolecular interactions: hydrogen bond (HB), hydrophobicity (ph), Aromatic-Aromatic (Ar-Ar), and Acceptor-Acceptor (AA) of the investigated compounds for Thumb pocket-I(site A), II(siteB), Palm pocket-I(site C) and the active site(AS) versus binding energy before and after adding RESP charge.

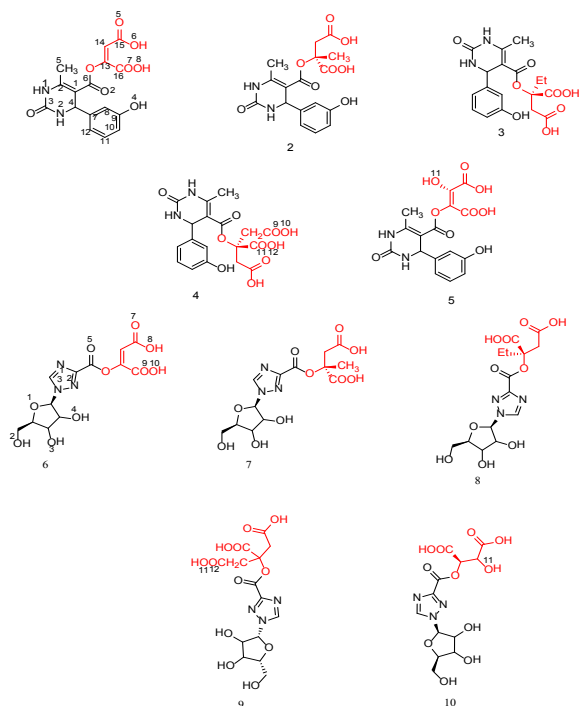


Fig.1

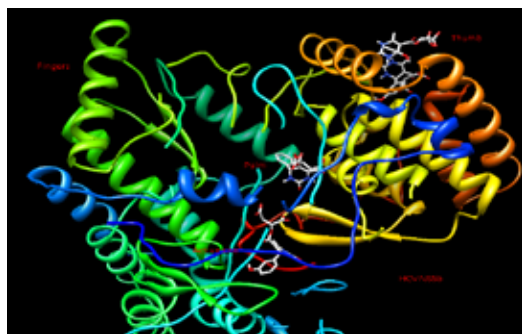


Fig.2

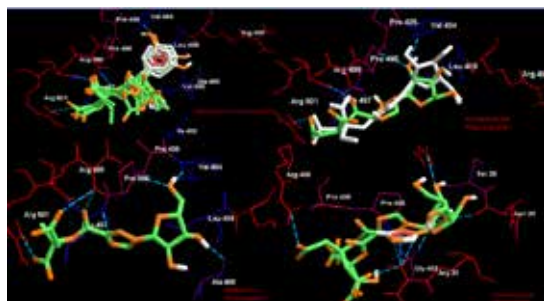


Fig.3

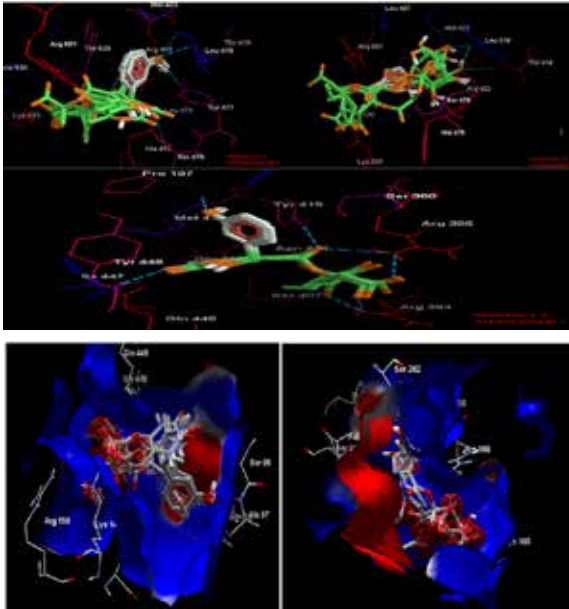


Fig.3: continued

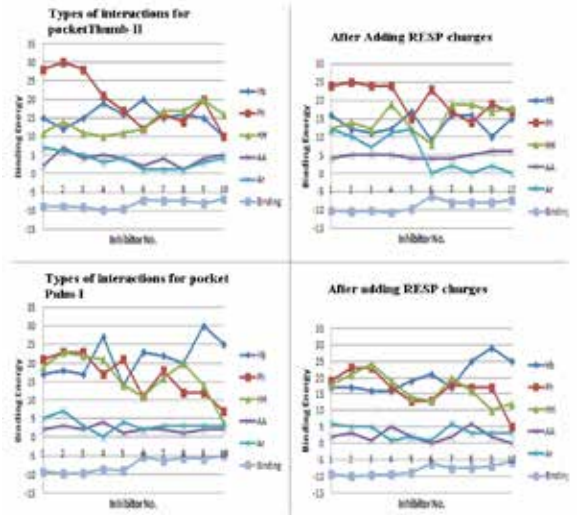


Fig. 4: Continued

Table 1: Correlation coefficient (R^2) for hydrophobicity (ph), hydrogen bond (HB) versus predicted free energy (Fe). Docking calculations done by Autodock before and after adding RESP charge.

Correlation type	Thumb pocket-I	Active Site	Thumb pocket-II	Palm pocket-I
Non nucleoside inhibitors : 1-5				
Neutral_Ph	0.43	0.41	0.77	0.85
Deprotonated_Ph	0.68	0.63	0.7	0.88
Neutral_HB	0.33	0.73	0.73	0.25
Deprotonated_HB	0.21	0.13	0.51	0.45
Nucleoside inhibitors: 6-10				
Neutral_Ph	0.89	0.86	0.91	0.90
Deprotonated_Ph	0.78	0.70	0.70	0.87
Neutral_HB	0.38	0.09	0.06	0.003
Deprotonated_HB	0.54	0.14	0.46	0.04

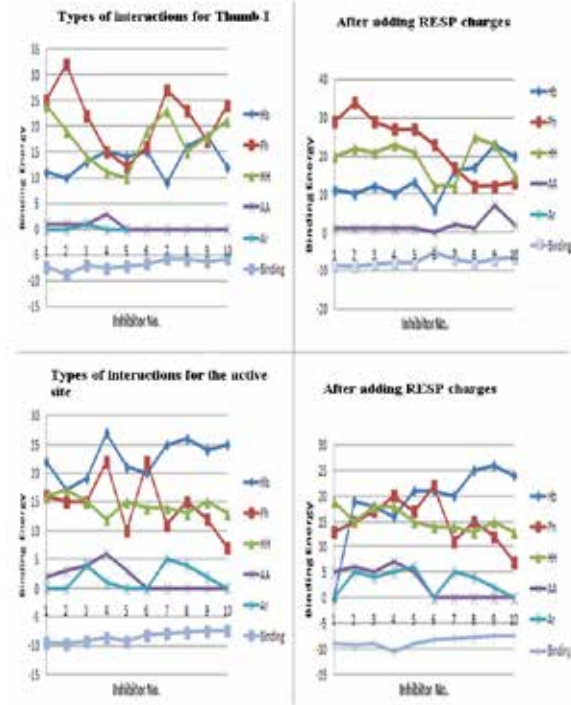


Figure 4

REFERENCE

- Beaulieu, P. L. (2009). Recent advances in the development of NS5B polymerase inhibitors for the treatment of hepatitis C virus infection. *Expert Opin Ther Pat*, 19(2), 145-164. | Betzi, S., Eydoux, C., Bussetta, C., Blemont, M., Leyssen, P., Debarnot, C., et al. (2009). Identification of allosteric inhibitors blocking the hepatitis C virus polymerase NS5B in the RNA synthesis initiation step. *Antiviral Res.*, 84(1), 48-59. | Bougie, I., & Martin, B. (2003). Initial binding of the broad spectrum antiviral nucleoside ribavirin to the Hepatitis C virus RNA polymerase. *The journal of biological chemistry*, 278(52), 52471-52478. | Brautigam, C. A., & Steitz, T. A. (1998). Structural and functional insights provided by crystal structures of DNA polymerases and their substrate complexes. *Curr. Opin. Struct. Biol.*, 8, 54-63. | Case, D. A., Darden, T. A., Cheatham, T. E., Simmerling, C. L., Wang, J., Duke, R. E., et al. (2010). AMBER11, University of California, San Francisco. | Chung, D. H., Sun, Y., Parker, W. B., Arterburn, J. B., Bartolucci, A., & Jonsson, C. B. (2007). Ribavirin reveals a lethal threshold of allowable mutation frequency for Hantaan virus. *Journal of virology*, 11722-11729. | Corouge, M., & Pol, S. (2011). New treatments for chronic hepatitis C virus infection. *Médecine et Maladies Infectieuses*(0). | Cosconati, S., Forli, S., Perryman, A. L., Harris, R., Goodsell, D. S., & Olson, A. J. (2010). Virtual screening with AutoDock: Theory and Practice. *Expert Opin Drug Discov.*, 5(1), 597-607. | El Bialy, S. A. A., Holger, B., & Lutz, F. T. (2005). Enantioselective synthesis of α -alkylmalates as the pharmacophoric group of several natural alkaloids and glycosides. *European Journal of Organic Chemistry*, 2005(14), 2965-2972. | Forli, S. (2010). Raccoon|AutoDock VS: an automated tool for preparing AutoDock virtual screenings. <http://autodock.scripps.edu/resources/raccoon> | Frisch, M. J., Trucks, G. W., Schlegel, H. B., Scuseria, G. E., Rob, M. A., Cheeseman, J. R., et al. | Gilbert, B. E., & McLeay, M. T. (2008). MegaRibavirin aerosol for the treatment of influenza A virus infections in mice. *Antiviral Research* 78, 223-229. | Gorbalenya, A. E., Pringle, F. M., Zeddard, J. L., Luke, B. T., Cameron, C. E., Kalmakoff, J., et al. (2002). The palm subdomain-based active site is internally permuted in viral RNA-dependent RNA polymerases of an ancient lineage. *J. Mol. Biol.*, 324, 47-62. | Hofmann, W. P., Herrmann, E., Sarrazin, C., & Zeuzem, S. (2008). Ribavirin modeofaction in chronic hepatitis C: from clinical use back to molecular mechanisms. *Liver International* 1478-3223. | Hou, T., Zhang, W., & Xu, X. (2002). Molecular docking studies of a group of hydroxamate inhibitors with gelatinase-A by molecular dynamics. *J Comput Aided Mol Des*, 16, 27-41. | Koren, G., King, S., Knowles, S., & Phillips, E. (2003). Ribavirin in the treatment of SARS: a new trick for an old drug? *Canadian Medical Association*, 168 (10), 1289-1292. | Kyte, J., & Doolittle, R. F. (1982). A simple method for displaying the hydrophobic character of a protein. *J Mol Biol*, 157(1), 105-132. | Lee, H. (2004). Mechanisms of Hepatitis C virus genome replication. *Stony Brook University*. | Lesburg, C. A., Radfar, R., & Weber, P. C. (2000). Recent advances in the analysis of HCV NS5B RNA-dependent RNA polymerase. *Curr. Opin. Investig. Drugs.*, 1(3), 289-296. | Li, H., Tatlock, J., Linton, A., Gonzalez, J., Borchardt, A., Dragovich, P., et al. (2006). Identification and structure-based optimization of novel dihydropyrones as potent HCV RNA polymerase inhibitors. *Bioorg. Med. Chem. Lett.*, 16, 4834-4838. | Mezei, M., & Zhou, M. M. (2010). Dockers: a computer program that analyzes the output of virtual screening of small molecules. *Source code for biology and medicine*, 5, 2. | Miles, D. L., Miles, D. W., Redington, P., & Eyring, H. (1976). Theoretical studies of the conformational properties of ribavirin. *Proc. Natl. Acad. Sci. USA*, 73(12), 4257-4260. | Moreno-Cid, A., Yebra, M. C., & Santos, X. (2004). Flow injection determinations of citric acid: a review. *Talanta*, 63(3), 509-514. | Moriyama, K., Suzuki, T., Negishi, K., Graci, J. D., Thompson, C. N., Cameron, C. E., et al. (2008). Effects of introduction of hydrophobic group on ribavirin base on mutation induction and anti-RNA viral activity. *J. Med. Chem.*, 51, 159-166. | O'Reilly, E. K., & Kao, C. C. (1998). Analysis of RNA-dependent RNA polymerase structure and function as guided by known polymerase structures and computer predictions of secondary structure. *Virology* 252, 287-303. | Pettersen, E. F., Goddard, T., Huang, C., Couch, G. S., Greenblatt, D. M., Meng, E. C., et al. (2004). UCSF Chimera: a visualization system for exploratory research and analysis. *J. Comput. Chem.*, 25(13), 1605-1612. | Ryška, J. (2011). Docking study of matrix metalloproteinase inhibitors. *Masaryk University, Brno.* | Sanner, M. F. (1999). Python: a programming language for software integration and development. *J. Mol. Graphics Mod*, 17, 57-61. | Shaw, W. (2008). Biological Treatments for Autism and PDD. | Sobolev, V., Sorokine, A., Prilusky, J., Abola, E. E., & Edelman, M. (1999). Automated analysis of interatomic contacts in proteins. *Bioinformatics*, 15(4), 327-332. | Thomsen, R., & Christensen, M. H. (2006). MolDock: A New Technique for High-Accuracy Molecular Docking. *J. Med. Chem.*, 49(11), 3315-3321. | Tietze, L. F., Braun, H., Steck, P. L., El Bialy, S. A. A., Tölle, N., & Düfert, A. (2007). Efficient synthesis of cephalotaxine- and deoxyharringtonine analogues by a trimethylaluminum-mediated domino reaction. *Tetrahedron*, 63(28), 6437-6445. | Véronique, L. R., Paul, C., Annick, R., Marianne, M., Gérard, B., Sophie, A., et al. (2011). Pharmacological exposure to ribavirin: A key player in the complex network of factors implicated in virological response and anaemia in hepatitis C treatment. *Digestive and Liver Disease*, 43(11), 850-855. | Wang, J., Cieplak, P., & Kollman, P. A. (2000). How well does a restrained electrostatic potential (RESP) model perform in calculating conformational energies of organic and biological molecules? *J Comput Chem*, 21(12), 1049-1074. | Yong, K.-C., Lindsay, K. L., Lee, K.-J., Lu, W.-C., He, J.-W., Milstein, S. L., Lai, M. M. C. (2003). Identification of a ribavirin-resistant NS5B mutation of Hepatitis C virus during ribavirin monotherapy. *Hepatology*, 869-878. | Zapata-Torres, G., Fierro, A., Miranda-Rojas, S., Guajardo, C., Saez-Briones, P., Salgado, J. C., et al. (2012). Influence of protonation on substrate and inhibitor interactions at the active site of human monoamine oxidase-a. *J Chem Inf Model*, 52(5), 1213-1221. | Zhou, X. X., Jahansson, N. G., & Wahling, H. (2005). Treatment of viral infections using prodrugs of 2',3-Dideoxy, 3' Fluoroguanosine, United States Patent (Vol. US 6,974,802 B2, pp. 198): Medivir, AB.